

Seeing Star Formation Regions with Gravitational Microlensing

Rodrigo Gil-Merino¹ & Geraint F. Lewis²

Institute of Astronomy, School of Physics, University of Sydney, NSW 2006, Australia

ABSTRACT

We qualitatively study the effects of gravitational microlensing on our view of unresolved extragalactic star formation regions. Using a general gravitational microlensing configuration, we perform a number of simulations that reveal that specific imprints of the star forming region are imprinted, both photometrically and spectroscopically, upon observations. Such observations have the potential to reveal the nature and size of these star forming regions, through the degree of variability observed in a monitoring campaign, and hence resolve the star formation regions in distant galaxies which are too small to be probed via more standard techniques.

Subject headings: gravitational lensing – microlensing – star forming regions – dark halo populations

1. Introduction

Gravitational microlensing is now a well established technique for the investigation of the distribution of compact (dark) matter in the universe. Furthermore, it also provides a powerful tool to study unresolved sources, such as in the case of the structure of QSOs, through temporal differential magnification (e.g. Yonehara et al. 1998).

From an observer's point of view, gravitational microlensing can be naturally divided in two different regimes. In the case of Galactic microlensing, the optical depth is low and a single star microlenses another star within the Galactic halo or in one of the galaxies in the Local Group (Paczynski 1986a). With Extragalactic microlensing, where the light from a distant quasar shines through a closer galaxy, the optical depth is roughly unity and many stars contribute to the overall microlensing effect (Paczynski 1986b). This paper considers this latter regime, where the source region is populated by a number of hot, young stars in a star forming region. Such a situation will occur in strongly lensed, multiply imaged systems, such as the multiple images seen in galaxy clusters (Mellier 1999), or the case where a isolated galaxy gravitationally lenses a more

distant galaxy (i.e. Warren et al 1996).

In a similar vein, Lewis & Iбата (2001) investigated the effect of a cosmological distribution of compact objects on the surface brightness distributions of galaxies at $z < 0.5$, considering a small microlensing optical depth (≤ 0.04) and they determined that low-level fluctuations in surface brightness of $\sim 2\%$ should result. Lewis et al. (2000) extended that analysis to distant galaxies observed through galaxy clusters, assuming dark matter to be composed of compact objects. Focusing upon Abell 370 as a case study, concluding that for low-luminosity ($\sim 10^4 L_\odot$) stellar populations would show rapid fluctuations exceeding 10% of the mean in the highest cases.

In this contribution we address the question of what microlensing signatures should be apparent in the case of part of a galaxy which is lensed by another galaxy. In particular, if the lensed parts of the source galaxy are regions of star formation, highly dominated by young, massive stars. Such a situation was recent presented by Smith et al. (2005) who reported the discovery of a new strong gravitationally lensed system, with an elliptical galaxy acting as the lens. The lens galaxy in this system is at redshift $z = 0.0345$ and the source, proposed to be a star formation region, is at $z \sim 0.45$, with the arcs formed by the gravitational mirage showing 'knots' of an extreme blue

¹rodrigo@physics.usyd.edu.au

²gfl@physics.usyd.edu.au

color of $B - I_c = 1.1$ (extinction corrected). This discovery poses the idea that microlensing in the multiple images of these systems might be able to distinguish the type of source stars involved in the mirage and help in the interpretation of its nature.

Within the context of gravitational lensing, a star formation region would appear as a non-uniform source, composed of a number of bright points in a more extended background. Hence, the microlensing imprint of such a source should show quite a different variability imprint from the uniform sources typically considered in gravitational microlensing experiments. The nature of this imprint is the basis of this current contribution.

2. Microlensing simulations

For the purpose of this study we performed microlensing simulations by means of ray-shooting techniques (Paczynski 1986b, Schneider & Weiss 1987, Kayser et al. 1986, Wambsganss 1990, Witt 1993, Lewis et al. 1993). To compute magnification patterns, one has to select certain values for the convergence (κ), which represents the gravitational potential due to matter in the beam, and the shear (γ), which is the perturbation to the beam due to the large scale distribution of matter. Typically, these parameters are drawn from a lens model for a particular system. For this study, however, representative values of $\kappa = 0.55$ and $\gamma = 0.55$ are employed, following Schechter et al. (2004), although other combinations would illustrate the situation equally; κ here includes also any form of compact dark matter, the effects of an smooth dark matter component are described in Schechter & Wambsganss (2002). Since high resolution maps are required, we used a receiving field of 2 Einstein radii¹, covered by a 2048^2 pixels area. The microlenses were randomly distributed and selected to have the same mass, $M_{\mu lens} = 1M_{\odot}$. Again, the selection of the mass range is arbitrary for our purposes. However, it is important to note that rather than covering a large area in the simulations, the key point remains in the resolution of the magnification patterns, be-

cause we are interested in small flux changes from pixel to pixel, so we also selected a high number of rays that resulted in over 700 per pixel on average.

The next step in the simulations is introducing the effect of the source. To do this, we assumed a source plane at $z = 0.5$ and two different sizes of 0.1 and 0.5 Einstein radii (ER), which corresponds to a physical size of 0.02 pc and 0.1 pc respectively at that distance for the standard Λ CDM cosmology. Although star formation regions might be larger than the bigger size considered, these two examples will illustrate the different effects due to their sizes and could be seen as clumps of star formations within larger regions (compact and ultra-compact H II regions as indicators of star formation might be <0.1 pc, see e.g. Gieveon et al. 2005 and references therein). We also assumed that our lens plane is at $z = 0.04$ (following the case of Smith et al. 2005). Depending on the stellar density of the source region, the number of stars in that region can vary from just a few up to hundreds. Considering first the 0.1 Einstein radii region, we ‘built’ three different sources: one containing 8 stars, another containing 80, and the last one as a uniform source, i.e., containing one star per pixel in the region (the number of stars are not representative of any particular region, and have been chosen arbitrarily).

The results for the first region size are displayed in Fig. 1. The upper left-hand panel corresponds to a ~ 1 ER² region of the original magnification pattern. The upper right-hand panel is the magnification pattern convolved with a region of 0.1 ER containing 8 stars. The lower right-hand panel is the same as the previous one but containing 80 stars. The lower left-hand panel is the magnification pattern convolved with an ‘uniform’ source of the same physical size.

In all the panels the same track has been drawn, in order to compare the synthetical light curves to each other; these are depicted in Fig. 2. The light curves are ~ 1 ER long, showing the different expected fluctuations corresponding to the different scenarios. The magnification distributions for the magnification patterns corresponding to the different panels in Fig. 1 are shown in Fig. 3. Clearly the number of stars in the region has a significant influence on the resulting light curve; in effect, the presence of each star produces a “shift-and-add” to the magnification map, greatly

¹The Einstein radius is defined in the source plane as $ER = \sqrt{4GM/c^2}(D_s D_{ls}/D_l)$, where M is the mass of the microlens, D is the angular distance to the source (s), the lens (l) and between the lens and the source (ls), c is the velocity of light and G the gravitational constant

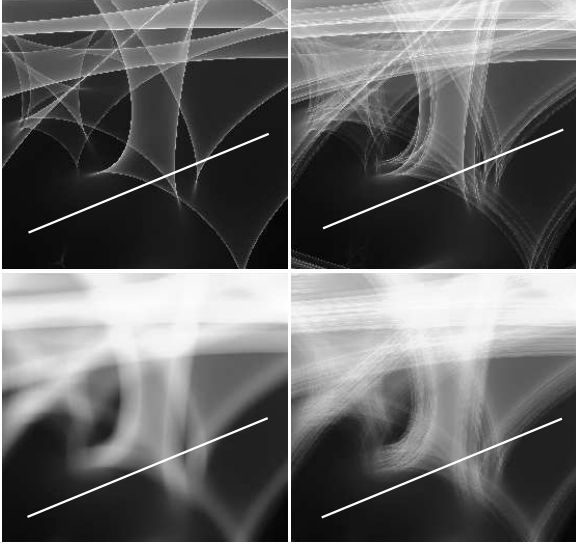


Fig. 1.— The original magnification pattern (upper left panel) is convolved with a field of 8 stars (upper right panel), 80 stars (lower right panel) and a ‘uniform source’ (lower left panel). The magnification map is 1 ER on a side.

increasing the number and overall density of caustics. This is reflected as additional peaks in the light curve. As the number of stars is increased to 80, some of the caustic structure has begun to wash out, leaving small scale fluctuations superimposed on a more gentle background, whereas the smooth source (which can be thought of as a very high density of stars) has washed out all small scale detail.

In Fig. 4, for comparison, we consider a region size of 0.5 ER containing also 8 stars, 80 stars and a ‘uniform’ source in the same manner as in Fig. 1. The corresponding track shows a completely different light curves compare to Fig. 2 although their positions are the same, due to the new caustic structure of the magnification maps according to the different size of the region considered.

The interpretation of these figures: if the magnification pattern is convolved with a ‘uniform’ source profile (Fig. 1, lower left panel) the result is always a smoother pattern, with smooth transitions in the value of the magnification from pixel to pixel; if the source area is made of a number of point-like objects, the convolution will show many caustics slightly shifted one another, with no

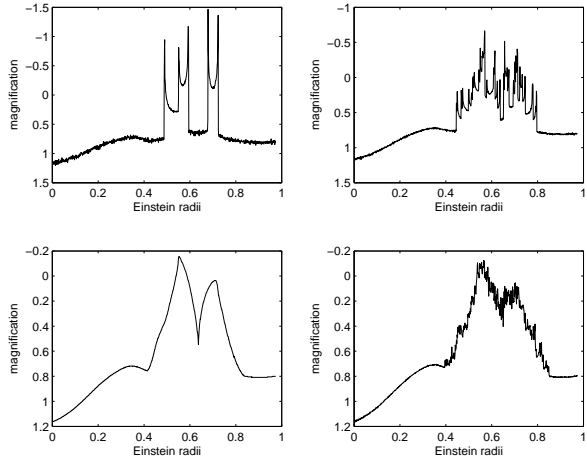


Fig. 2.— The corresponding synthetic light curves to the tracks plotted in Fig. 1. When a few stars dominate the source region (upper-right panel), the variability can be easily distinguish from a ‘uniform’ source (lower-left panel).

smooth transition between them. This translates into a rapid variability in the lightcurves of the corresponding source. Also, the size of the regions considered plays an active role in the final imprint of microlensing in the observational light curves.

3. Applications and Discussion

The application of the simulations described in the previous Section can be done in the following manner. If multiple lensed ‘knots’ are detected in an image (see, e.g., Fig. 3c in Smith et al. 2005) and are thought to be star-forming regions, the flux will be highly dominated by young O-stars. In principle, since young massive stars are rare due to their evolutionary process, only a few are expected in these star forming knots (an ultraviolet and optical spectral atlas of the Small Magellanic Cloud includes <20 O-stars, see Walborn et al. 2000). Observing these areas, e.g. in the UV band, which characterizes regions of star formation, with periodic photometry, the variability of the observed light curves will be related to the number and separation of these stars present in the star forming regions (the contamination by late-type stars in the UV will be almost null). In practice, one could treat the problem statistically by simulating the observed variability and thus put limits on the amount and luminosity of young dominating stars.

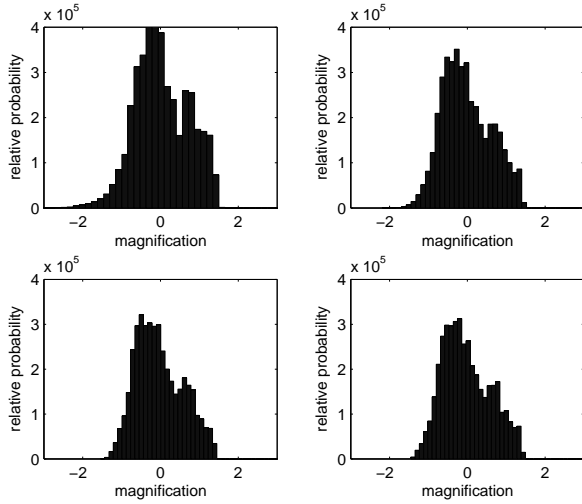


Fig. 3.— The relative probability distributions of the corresponding pannels in Fig. 1.

Knowing the luminosity of these stars accurately is important, because their masses derived by stellar evolutionary models and by stellar atmosphere models can be compared. Stellar evolution theory and initial mass function might take advantage of these results as well. Gravitational microlensing might be the only tool to ‘resolve’ these stars in clusters of star formation, otherwise impossible to investigate in galaxies at moderate/high redshift.

Spectroscopy of microlensed star-forming regions might help to put limits on their nature as well. Gravitational microlensing of broad spectral lines in QSOs has been studied theoretically by a number of authors (e.g., Abajas et al. 2002, Lewis et al. 2004, Richards et al. 2004) and used to put limits on the size of the broad line emitting regions of the QSOs. In those cases, the natural shape of a line is distorted by the complex net of caustics produced by the microlenses on the source plane. Since microlensing of the broad line region is expected when its physical size is of the order of the Einstein radius of the lens projected onto the source plane, microlensed spectral lines give an idea of such physical sizes. In the same way, observing typical spectral lines of O-stars (e.g. in the UV, O V $\lambda 1371\text{\AA}$, C III $\lambda 1176\text{\AA}$ in the optical, He II $\lambda 4686\text{\AA}$, N III $\lambda 4634\text{\AA}$ and $\lambda 4640\text{\AA}$) one would expect the lines to be deformed by the presence of the caustics (due to magnifications/demagnifications), and these variations in

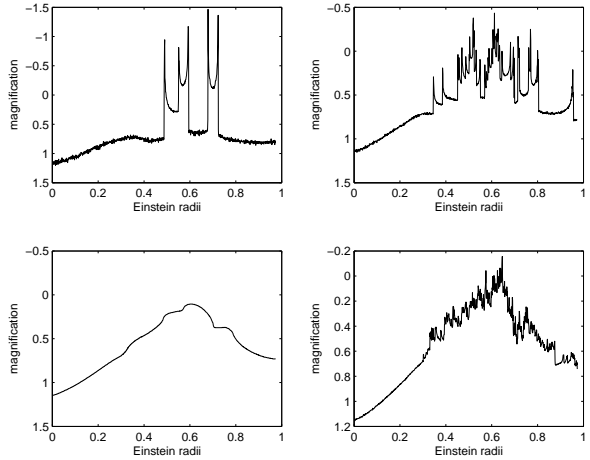


Fig. 4.— Light curves considering a region with a size of 0.5 ER.

the spectral lines might reveal the size and populations of the star forming regions.

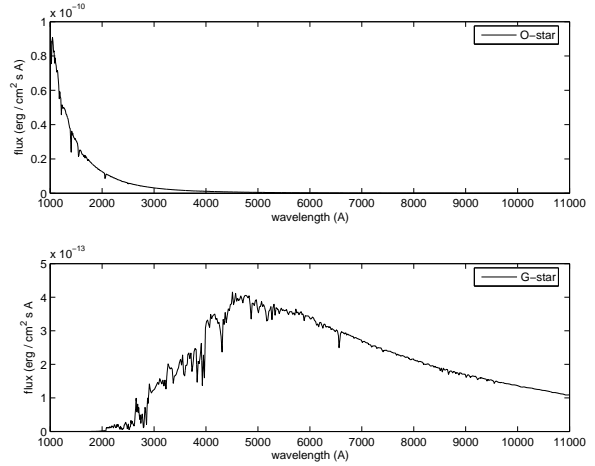


Fig. 5.— Spectra of O-star and G-star models. The contribution of a solar-type star to the total flux in the (far)UV band can be ignore, since it is several orders of magnitudes lower. See text for references.

To illustrate this, we plot in Fig. 5 the spectra of an O-star (upper panel) and a solar-like G-star (lower panel), obtained from the Kurucz models database². For any unresolved star formation region, the (far-)UV range of the spectrum will be dominated by these O-stars. Late-type stars fluxes

²http://garnet.stsci.edu/STIS/stis_models.html

in UV are several orders of magnitude lower and thus they do not contribute significantly to the total luminosity and the flux distribution in the upper panel of Fig. 5 might be a representative one for that part of the spectrum (different lines might be present, obviously). Microlensing affecting this part of the spectrum will only show an enhancement of the flux. However, the effect is slightly different when using optical range of the spectrum. In this case, the flux contribution due to late-type stars starts to be dominant, although O-stars flux is still significantly present. We construct a toy star formation region model, merging the spectra of the O-star and the G-star shown in Fig. 5, assuming that 90% of the total flux comes from solar-like stars and the rest is produced by early-type stars. The toy model is depicted in Fig. 6 (lower line, spectrum marked as 'O-star+G-star') showing only the 1500Å-5500Å wavelength interval. When the star formation region travels across the magnification pattern in Fig. 1, late-type stars will act as a constant flux background as a whole and microlensing will affect mainly O-stars. In this way, the microlensing signature in the spectra will be a flux ratio variation between O-stars and late-type stars spectral lines. This is shown also in Fig. 6 (upper line, spectrum marked as 'O-star+G-star+microlensing'). There is not only an enhancement of the flux in the bluest part of the spectrum, but also a deformation of certain lines due to the different microlensing effect on the different type of stars. In Fig. 7 and Fig. 8 we repeat the procedure, but assuming a different relative flux between the two types of stars. In Fig. 7, 1% of the flux is coming from O-type stars and 99% is from late-type stars; in Fig. 8 the percentage is 0.1% and 99.9% for early and late-type stars respectively. As shown in Fig. 2, high variability is expected. Both Figures 3 and 2 show that the amount of variability depends on the nature of the star formation regions (number of stars, size of the regions...). This means that comparing several consecutive spectra one would be able to statistically determine the relative flux variability of the spectral lines and continuum due to the presence of the caustics, and thus compare them with the expected one from the simulations, putting limits to the number and distribution of the early-type stars.

A key point to note is that to detect these mi-

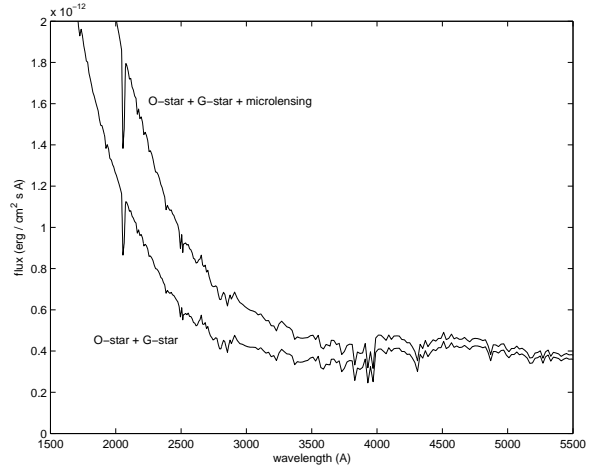


Fig. 6.— The toy model for a star formation region is made of two superimposed spectra of a O-star and a G-star. The relative flux between the two types of stars is 10% and 90% for the O-type and G-type respectively. We introduce the microlensing effect as an enhancement in the flux of the O-stars by a factor of 1.6, which corresponds to a decrease of 0.5 magnitudes (upper line).

cro lensing effects on star formation regions is the time scale of the events. Considering the lens configuration describe in Sec. 2, we can estimate a typical separation between microcaustics in the magnification maps in Fig. 2. This separation is ~ 0.005 ER for the upper right-hand panel, which corresponds to approximately 10^{-3} pc. Assuming a transverse velocity for the source galaxy of ~ 6000 km/s (see Kayser et al. 1986), the resulting time-scale for the events is ~ 50 days. The time-scales of the events get shorter when the number of O-stars gets higher, although the flux variability is smaller. This means that six data points in a time period of around three months should be able to described the type of variability involved in the gravitational microlensing scenario.

4. Conclusions

We described in this contribution how to apply gravitational microlensing to the observations of unresolved extragalactic star forming regions. The discussion shows that due to the caustics configuration in the magnification maps of the region, rapid monitoring campaigns, both photometric or spectroscopic, would reveal high variability fluctu-

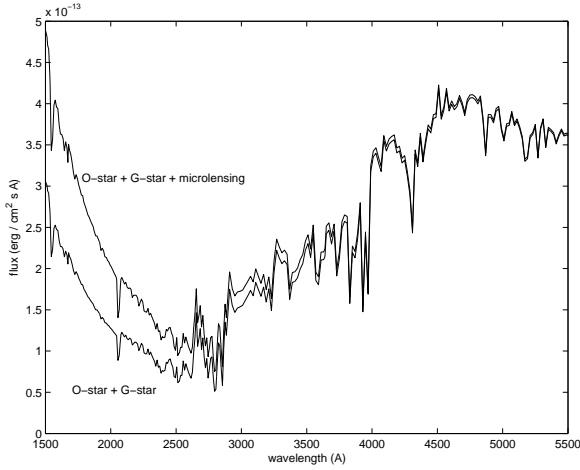


Fig. 7.— As Fig. 6 but the flux contribution is 1% and 99% from the O-star and the G-star respectively.

ations due to the number of early-type stars. The specific amount of variability will depend on the number of stars and their distribution in the region, as well as on the exact configuration of the microlenses in the lensing galaxy. Thus, the study of a particular system requires the knowledge of a lens model to perform the right simulations and the analysis of the results should be based on a statistical approach. The advantage of the method, if these circumstances take effect, is that we might be able to investigate star formation regions which are difficult to analyse with more traditional techniques.

REFERENCES

- Abajas C., Mediavilla E., Muñoz J.A., Popović L.Ć., Oscoz A., 2002, *ApJ*, 576, 640
- Bagherpour H., Branch D., Kantowski R., *astro-ph/0503460*
- Giveon U., Becker R.H., Helfand D.J., White R.L., 2005, *ApJ*, 129, 348
- Kayser R., Refsdal S., Stabell R., 1986, *A&A*, 166, 36
- Haser S.M., Pauldrach A.W.A., Lennon D.J. et al., 1998, *A&A*, 330, 285
- Heap S.R., Lanz T., Hubeny I., 2004, *astro-ph/0412345*

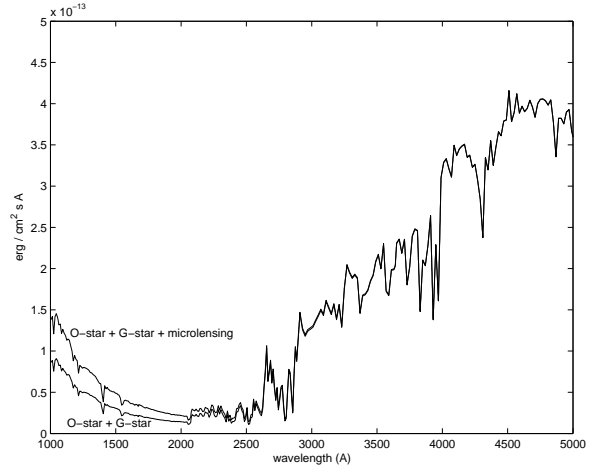


Fig. 8.— As Fig. 6 but the flux contribution is 0.1% and 99.9% from the O-star and the G-star respectively.

- Lewis G.F., Ibata R.A., 2001, *ApJ*, 549, 46
- Lewis G.F., Ibata R.A., 2004, *MNRAS*, 348, 24
- Lewis G.F., Ibata R.A., Wyithe J.S.B., 2000, *ApJL*, 452, L9
- Lewis G.F., Miralda-Escudé J., Richardson D.C., Wambsganss J., 1993, *MNRAS*, 283, 647
- Mellier Y., 1999, *ARA&A*, 37, 127
- Paczynski B., 1986a, *ApJ*, 304, 1
- Paczynski B., 1986b, *ApJ*, 301, 503
- Richards G.T., Keeton C.R., Pindor B. et al., 2004, *ApJ*, 610, 679
- Schechter P.L., Wambsganss J., 2002, *ApJ*, 580, 685
- Schechter P.L., Wambsganss J., Lewis G.F., 2004, *ApJ*, 613, 77
- Schneider P., Weiss A., 1987, *A&A*, 171, 49
- Smith R.J., Blakeslee J.P., Lucey J.R., Tonry J., 2005, *ApJ*, accepted (*astro-ph/0504453*)
- Walborn N.R., Lennon D., Heap S.R. et al., 2000, *PASP*, 112, 1243
- Wambsganss J., 1990, Ph.D. thesis, Munich Univ. Report MPA550

Witt H.J., 1993, ApJ, 403, 530

Yonehara A., Mineshige S., Manmoto T. et al.,
1998, ApJ, 501, 41